Assessing the dispersion of supported H3PW12O40 catalysts: No longer a hurdle thanks to in situ IR upon pyridine adsorption

Josefine Schnee, François Devred, Eric M. Gaigneaux, Alexandre Vimont

Assessing the dispersion of supported $H_3PW_{12}O_{40}$ catalysts: no longer a hurdle thanks to *in situ* IR upon pyridine adsorption

Josefine Schnee,[1]* François Devred,[2] Eric M. Gaigneaux,[2] Alexandre Vimont,[1]*

[1]Normandie Université, ENSICAEN, UNICAEN, CNRS, Laboratoire Catalyse et Spectrochimie, 14000 Caen, France
[2]Institute of Condensed Matter and Nanosciences (IMCN) – Molecular Chemistry, Materials and Catalysis (MOST) – Université catholique de Louvain (UCL), Place Louis Pasteur 1, box L4.01.09 1348 Louvain-la-Neuve, Belgium

*Corresponding authors. E-mail addresses: josischnee@hotmail.com, alexandre.vimont@ensicaen.fr

Abstract

Pyridine is since a long time used as an infrared (IR) molecular probe to characterize the acidity of solids, in particular of heteropolyacids (HPAs). The latter are metal-oxygen-clusters nowadays widely used in acid catalysis. Indeed, thanks to their exceptionally strong Brönsted acidity, they allow operating chemical reactions under significantly milder conditions than required by conventional catalysts. In the case of $H_3PW_{12}O_{40}$, the most acidic Keggin-type HPA, it is well-known that the exposure to pyridine leads to an unusual IR spectrum. Indeed, the band at about 1540 cm^{-1} associated to the ν_{19b} pyridinium ring stretch mode is split in two. Up to now, this phenomenon was studied with the only aim of understanding its origin, which was proposed to be a tunneling effect related to a frustrated rotation of the pyridinium cation within the solid bulk of $H_3PW_{12}O_{40}$. Here, we demonstrate for the first time that it can actually be used as an analytical tool, namely to probe the degree of dispersion of supported $H_3PW_{12}O_{40}$ units, a key parameter dictating their catalytic performance. We support $H_3PW_{12}O_{40}$ on TiO_2 P25 (hydrophilic) and TiO_2 T805 (hydrophobic), so yielding samples with different degrees of dispersion, as qualitatively assessed through X-ray photoelectron spectroscopy. Through *in situ* Fourier-transform IR spectroscopy upon pyridine adsorption, we show that the ν_{19b} pyridinium vibration band only and systematically splits in the presence of agglomerated Keggin units. More precisely, the higher the fraction of agglomerated Keggin units, the more marked the band splitting. So, the latter appears as a fingerprint of agglomerated $H_3PW_{12}O_{40}$. Furthermore, following an easy treatment, the IR spectra allow quantitatively evaluating the fractions of dispersed *vs.* agglomerated Keggin units within the samples, which is very difficult to achieve through any other technique.

Keywords: FT-IR spectroscopy; *In situ* monitoring; Pyridine adsorption; Keggin heteropolyacid; Supported catalysts; Dispersion

1. Introduction

Pyridine is nowadays widely used as a probe molecule to characterize the acidity of solids (both in terms of number and type/strength of the acid sites).[1,2,3,4] Indeed, it adsorbs onto the acid sites and, depending on whether these are of Lewis or Brönsted type, it forms a different species being detectable/quantifiable through infrared (IR) spectroscopy.[2,3,4] In the case of Brönsted acid sites, a pyridinium cation (PyH^+) is formed, which has its main IR fingerprint band at about 1540 cm^{-1} (a position being independent of the nature of the counter-anion).[1] The latter band is associated to the vibration of the pyridinium ring in the stretch mode noted "ν_{19b}" (the "b" referring to the symmetry type B_2 to

which this vibration mode belongs following the group theory, with the pyridinium cation being characterized by a C_{2v} point group of symmetry elements).[1]

For conventional solids, the pyridine-IR characterization is limited to the only surface. However, in the case of heteropolyacids (HPAs), standing at the heart of the present work, the situation is different. HPAs are metal-oxygen clusters that are nowadays widely used in acid catalysis. Thanks to their exceptionally strong Brönsted acidity, they generally allow operating chemical reactions under significantly milder conditions than required by conventional acid catalysts (e.g. alumina or zeolites).[5] The most easily available HPAs are those having the Keggin structure. Described by the general formula $H_nXM_{12}O_{40}$, they contain $[XM_{12}O_{40}]^{n-}$ heteropolyanions stabilized by n acidic protons, with X being the heteroatom (often P^{V}, Si^{IV}) and M being the addenda atom (transition metal, typically Mo^{VI}, W^{VI}).[6] More precisely, the heteropolyanions are made of a central XO_4 tetrahedron, surrounded by twelve MO_6 octahedra. They contain three types of oxygen atoms: central (O_a), bridging, and terminal (O_t) ones. The bridging ones are either corner-sharing (O_b) or edge-sharing (O_c).[6,7]
HPAs exhibit a so-called "pseudo-liquid" behavior. This means that they absorb polar (and relatively small) molecules such as alcohols, ethers or pyridine into their solid bulk, thus in-between their constitutive heteropolyanions.[8,9,10,11] In the case of pyridine, this leads to the formation of a pyridinium salt.[12,13,14] So, pyridine probes not only the acid sites located at the surface of HPA crystals but also those located within their bulk.

In the case of $H_3PW_{12}O_{40}$, the most acidic Keggin HPA, the pyridinium salt gives rise to an unusual IR fingerprint. Indeed, its ν_{19b} band is split in two (as well as its ν_{8b} band centered at about 1610 cm^{-1}).[1,15,16] The most likely explanation for this phenomenon is the following.[1] In the solid bulk, the pyridinium ring is sterically hindered from rotating around the axis joining the center of the ring to the O_t atom of the heteropolyanion to which the pyridinium cation is bonded. This frustration leads to an in-plane rotation of the pyridinium cation towards another type of oxygen atom, namely an O_c one, through a tunneling effect. So, the pyridinium cation actually switches between two positions differing by the type of oxygen atom of the heteropolyanion to which it is H-bonded. This switch splits the δN^+-H energy levels, and, as they present a particularly marked δN^+-H character, the ν_{19b} and ν_{8b} ring vibration modes as well. In other words, the frustrated in-plane rotation of the pyridinium ring appears as an additional mode, which is called the tunnelling mode. As a consequence, the IR bands resulting from the ν_{19b} and ν_{8b} modes contain two contributions and are split.

In the present work, we demonstrate for the first time that the above pyridinium IR band splitting can actually be exploited as an analytical tool. We support $H_3PW_{12}O_{40}$ on two different commercial TiO_2 supports. The first one is TiO_2 "P25" (20% rutile - 80% anatase), which is widely used as a support for HPAs in order to increase the accessibility of the individual units.[8,17,18,19] The second one is TiO_2 "T805", a hydrophobized version of TiO_2 P25, to our knowledge not yet used to support HPAs. The idea of using supports with different hydrophilicities is to obtain supported $H_3PW_{12}O_{40}$ samples with different degrees of dispersion, as recently achieved in reference[20]. If the pyridinium IR band splitting observed for bulk $H_3PW_{12}O_{40}$ really originates from a frustrated rotation of the pyridinium cation due to neighboring Keggin units, its extent in the case of supported $H_3PW_{12}O_{40}$ could possibly depend on whether the Keggin units are well-dispersed or agglomerated. In other words, the extent of the pyridinium IR band splitting could possibly be exploited as a tool to probe the dispersion of supported $H_3PW_{12}O_{40}$, namely a key parameter dictating their catalytic performance (as shown for example in the conversion of methanol to dimethylether[17,20]). The feasibility of this idea is precisely what we investigate in the present work, by combining *in situ* Fourier-transform infrared (FT-IR) spectroscopy

upon pyridine adsorption with the commonly used[17,20] techniques to assess the dispersion of HPAs, namely X-ray photoelectron spectroscopy (XPS) and X-ray diffraction (XRD).

2. Experimental

2.1. Preparation of the supported $H_3PW_{12}O_{40}$

TiO_2 P25 and T805 were purchased from Evonik Industries (AEROXIDE® TiO_2 P25 and T805). TiO_2 T805 is a fumed titanium dioxide that was treated with octylsilane to achieve a hydrophobic surface (C-content of 2.7 - 3.7 wt.% according to Evonik's Product Information Sheet[21]). $H_3PW_{12}O_{40}$ (hereafter HPW12) was purchased from Sigma-Aldrich in the form of $H_3PW_{12}O_{40}.xH_2O$ (reagent grade). It was supported on both TiO_2 supports by wet impregnation at room temperature. Precisely, the appropriate amounts of HPW12 (corresponding to the nominal loadings/weight fractions provided in Table S1 in the Supporting information) were dissolved in ethanol (AnalaR NORMAPUR®, > 99,8%) and then added dropwise to 1 g of support dispersed also in ethanol. The resulting mixtures were stirred for 2 hours, before the solvent was evaporated in a rotary evaporator at 40 °C. Finally, the samples were dried overnight in a vacuum oven (< 40 Torr) at room temperature.

The real HPW12 loadings were determined through inductively coupled plasma atomic emission spectrometry (ICP-AES) with an ICAP 6500 Thermo Scientific apparatus. The values are provided together with the nominal loadings in Table S1, being expressed both in weight fractions and in "% ML" (and plotted against the nominal loadings on Figure S1). The latter unit means the percentage of the total amount of Keggin units theoretically required to cover the supports with one ideal monolayer (abbreviated here to "ML"). Hereafter, all results are discussed with respect to the real HPW12 loadings, and the latter are expressed in % ML to get rid of the difference in specific surface area of the two TiO_2 supports (45 *vs.* 33 m^2/g respectively for P25 *vs.* T805) when comparing the supported samples in terms of HPW12 dispersion. The specific surface area of the supports was measured with a Micromeritics Tristar Surface Area and Porosity Analyser after having degassed the samples overnight at 150 °C under a vacuum of about 80 mTorr. As reflected by the N_2 physisorption isotherms provided on Figure S2 in the Supporting information, both supports are exclusively macroporous. They do not contain micro- or mesopores. The loadings of HPW12 in % ML were calculated by considering that Keggin units are spherical and have a diameter of 1 nm.[22]

2.2. Assessment of the dispersion in the usual way

XPS was performed with a SSX 100/206 spectrometer from Surface Science Instruments (USA) equipped with a monochromatized and microfocused Al X-ray source (powered with 20 mA and 10 kV). The pressure within the analysis chamber was about 10^{-6} Pa. The angle between the normal to the surface and the axis of the input lens of the analyzer was 55°. The zone analyzed was about 1.4 mm^2 and the pass energy was set at 150 eV for the general spectra and at 50 eV for the elementary spectra. An electron gun set at 8 eV and a nickel grid placed 3 mm above the surface of the samples were used to stabilize the charge. The following sequence of spectra was recorded: general spectrum, C 1s, O 1s, Ti 2p, W 4d, and again C 1s to check the stability of the charge compensation as a function of time and the absence of sample degradation.

The elements were quantified by using the sensitivity factors and acquisition parameters provided by the manufacturer, after having set the binding energy scale by fixing the C-(C,H) component of the C 1s peak at 284.8 eV. The W/Ti ratio was plotted as a function of the loading of HPW12 on both TiO_2

supports. Indeed, such a plot directly reflects the way how HPW12 interacts with the supports. In general, the higher the W/Ti ratio, the more the Keggin units are dispersed over the surface of the support. In particular, a linear increase of the W/Ti ratio with the HPW12 loading (from the origin of the graph) reflects the formation of an ideal monolayer of Keggin units progressively covering the surface of the support. Any other tendency *vs.* the loading (i.e. a linear increase with a lower slope than needed to be aligned with the origin of the graph, a horizontal line, or a decrease) reflects the formation of aggregates.

Powder XRD patterns were measured at room temperature with a Kristalloflex Siemens D5000 diffractometer using the copper *K*α radiation (λ = 0.15418 nm) and being equipped with a scintillation detector. The X-ray source was operated with a tension of 40 kV and a current of 40 mA. The appearance or not of the diffraction lines observed for pure (thus crystalline) HPW12 on the XRD patterns of the supported samples was used as an indicator of respectively poor or good dispersion of the Keggin units.

2.3. In situ FT-IR upon pyridine adsorption-desorption

Samples were pressed into a self-supported disc (2 cm^2 area, 10 mg cm^{-2}). The resulting pellets were placed into a homemade IR cell which was equipped with KBr windows and connected to a vacuum line. The latter line served for evacuation steps, thermal treatments and introduction of small doses of pyridine vapor (typically 1 Torr). Thanks to a movable sample holder, the pellets were set alternatively into the IR beam for spectra acquisition at room temperature and into a furnace at the top of the cell for thermal treatments. The spectrometer was a Nicolet Nexus one equipped with a KBr beam splitter and a deuterated-triglycine sulfate (DTGS) detector. The FT-IR spectra were measured at 4 cm^{-1} resolution, and treated with the Thermo Scientific OMNIC software.

In a typical experiment, the sample was first pre-treated for 1 hour under vacuum (until reaching 10^{-6} Torr) at 100 °C to evacuate structural water. Indeed, Keggin HPAs are highly hygroscopic.[5] Then, it was exposed to 1 Torr of pyridine (non-deuterated h_5-one, 99+% grade from Aldrich), first at room temperature and then at 100 °C, both times for 1 hour. The step at 100 °C aimed at making pyridine diffuse into the bulk of potential HPW12 agglomerates. Finally, during pyridine evacuation (until reaching 10^{-6} Torr), the sample was first left at room temperature for 1 hour and then heated up to 100 °C, again for 1 hour (to check the stability of adsorbed pyridine). FT-IR spectra were measured at room temperature during and/or after every step (always after in the case of heating steps because of the setup configuration).

Whatever the sample, before pyridine adsorption, not any absorption band was observed around 1540 cm^{-1} where appears the ν_{19b} pyridinium ring vibration band of interest here. Upon exposure to pyridine, in the cases where the ν_{19b} band got split, it never did before heating to 100 °C. Moreover, upon evacuation of pyridine, the spectra before and after heating at 100 °C were always the same. For these reasons, the full sequence of spectra is shown here only for some chosen samples (those with the highest HPW12 loading on both supports, as well as pure TiO_2 P25 for reference) in the Supporting information (Figure S3). The Results and discussion section focuses on the spectra measured after heating to 100 °C in the evacuation period, as this stage ensures the absence of excess pyridine within the bulk of HPW12. Indeed, such an excess leads to variations of the ν_{19b} band intensity.[13]

Regarding the structure of HPW12, it was checked to be of Keggin type as in pure HPW12 for all the supported samples. Indeed, the characteristic bands at 1080 and 980 cm^{-1}, respectively associated[6] to P-O_a-W and W=O_t vibrations within the Keggin structure, were systematically observed (Figure S4).

3. Results and discussion

Figure 1 shows the surface atomic ratio of W over Ti as a function of the HPW12 loading on both TiO_2 supports (37, 66 and 82% ML on TiO_2 P25; 35, 49 and 67% ML on TiO_2 T805).

On TiO_2 P25, the W/Ti ratio systematically increases with the loading. The values at 37 and 66% ML are aligned with the origin of the graph, reflecting that the Keggin units within the two concerned samples are dispersed as an ideal monolayer over the support. Then, from 66 to 82% ML, the W/Ti ratio increases less than predicted by the line passing through the preceding points, reflecting the presence of agglomerated Keggin units at 82% ML. These observations are consistent with the work in reference[20].

On TiO_2 T805, the situation is much different. All three supported samples show relatively close W/Ti ratios, however with a decreasing tendency from one loading to the next. Moreover, the W/Ti ratios are all significantly lower (at least two times) than the lowest value observed with TiO_2 P25. All this indicates that, on TiO_2 T805, from the lowest loading, the Keggin units agglomerate/stack on each other (either starting from the support surface, or forming independent aggregates) instead of forming a well-dispersed layer over the support surface. The same kind of behavior was recently observed for HPW12 supported on hexagonal boron nitride (also hydrophobic). However, in that case, above a threshold loading of 40% ML, the Keggin units tended to penetrate into/disperse within the interlayers of boron nitride, making the W/Ti ratio increase again.[20] Here, on TiO_2 T805, the higher the HPW12 loading, the lower the W/Ti ratio, thus the higher the tendency of the Keggin units to interact with each other rather than with the support, and the lower the fraction of Keggin units dispersed over the surface of the support.

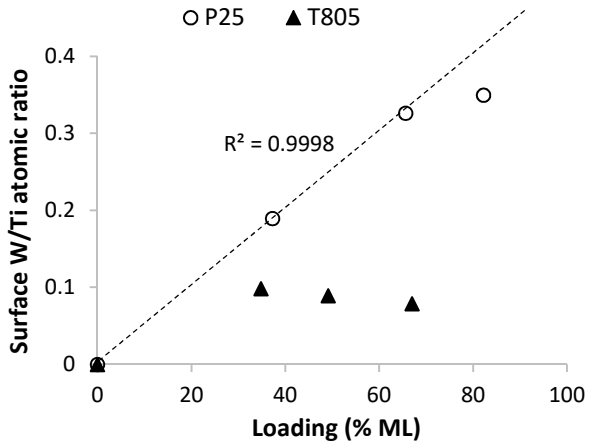

Figure 1. XPS-measured W/Ti surface atomic ratio as a function of the loading of HPW12 on TiO_2 P25 and T805. The R^2 applies to the dotted line passing through the first three points relative to TiO_2 P25, including the origin.

Figure 2 shows the FT-IR spectra of pyridine adsorbed onto the HPW12/P25 (Figure 2a) and HPW12/T805 (Figure 2b) samples. As a reference, Figure S3 in the Supporting information provides the spectra of pyridine adsorbed onto pure TiO_2, measured in the same conditions (the bands being assigned in the related text, according to reference[2]).

On Figure 2, the characteristic ν_{19b} pyridinium ring vibration band due to the protonation of pyridine by HPW12 emerges at around 1540 cm^{-1}. It is the only band being specific to pyridine interacting with HPW12. All the other bands are either 1) specific to pyridine adsorbed on TiO_2 (at 1575-1580 and 1445 cm^{-1}), or 2) they appear at a position where a contribution from pyridine adsorbed on TiO_2 may not be excluded (as witnessed by the spectra of pyridine adsorbed onto pure TiO_2 on Figure S3), or 3) they are

specific to the support itself (the band at 1466 cm^{-1} observed with T805 being associated to the deformation of methyl groups). So, the ν_{8b} pyridinium ring vibration band appearing at around 1610 cm^{-1} on the spectrum of pure $(PyH^+)_3(PW_{12}O_{40})^{3-}$ shown elsewhere[1] is masked here, and can thus not be considered. From integrating the ν_{19b} pyridinium ring vibration band of the spectra in Figure 2, and applying the Beer-Lambert law with an absorption coefficient of 1.36 μmol^{-1} cm (according to reference[23]) and a pellet surface of 2 cm^2, the number of pyridinium cations formed within the samples was estimated. This number nicely corresponds with the number of protons contained in the samples (Figure 3), which was calculated from the HPW12 loading, knowing that each Keggin unit possesses 3 protons. This correlation confirms that pyridine indeed probes the whole protons within the samples, whatever the HPW12 loading.

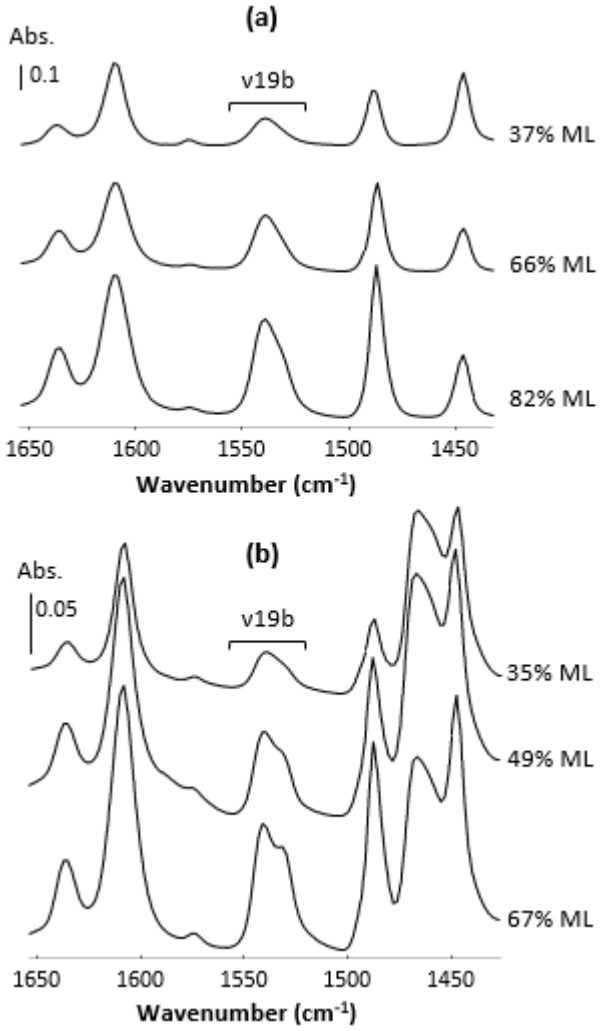

Figure 2. *In situ* FT-IR spectra of the HPW12/P25 (a) and HPW12/T805 (b) samples after exposure to pyridine, in the region of the ν_{19b} pyridinium ring stretch. They were measured at room temperature during pyridine evacuation out of the IR cell, precisely after 1 hour under vacuum at 100 °C. "Abs." means absorbance, and it is expressed in arbitrary units.

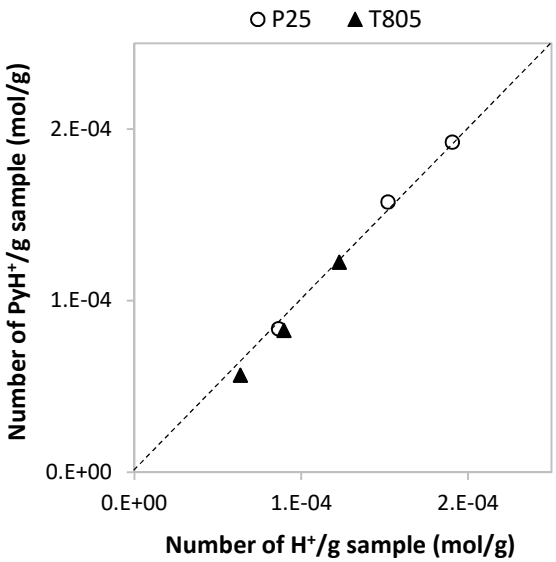

Figure 3. Number of pyridinium cations contained in the samples after exposure to pyridine (obtained by integrating the ν_{19b} pyridinium ring vibration band of the spectra in Figure 2, and by applying the Beer-Lambert law with an integrated absorption coefficient of 1.36 μmol^{-1} cm reported in reference[23] and a pellet surface of 2 cm^2) *versus* their number of protons (calculated from the HPW12 loadings, by considering that each Keggin unit possesses 3 protons).

In the case of the HPW12/P25 samples with 37 and 66% ML of HPW12 (containing well-dispersed Keggin units according to Figure 1), the ν_{19b} pyridinium ring vibration band is not split (Figure 2a). It has a single maximum at 1540 cm^{-1}. In the case of the HPW12/P25 sample with 82% ML (containing agglomerated Keggin units), the band shows a maximum at 1540 cm^{-1}, with a slight shoulder at 1530 cm^{-1} (Figure 2a). Regarding the HPW12/T805 samples (containing more and more poorly dispersed Keggin units with increasing loading), those with 49 and 67% ML both show a split ν_{19b} pyridinium ring vibration band, with the two maxima being located at 1540 and 1530 cm^{-1}. The sample with 35% ML also shows, next to its maximum at 1540 cm^{-1}, a shoulder at 1530 cm^{-1} (Figure 2b).

So, as long as the Keggin units are well-dispersed on the support, the ν_{19b} ring vibration band remains non-split. When agglomerated Keggin units are present (either because the loading was too much increased on TiO_2 P25, or because, at a given loading, TiO_2 T805 was used instead of TiO_2 P25), the band is systematically split. More precisely, the splitting occurs to an extent that depends on the fraction of agglomerated Keggin units. Indeed, on TiO_2 T805, the higher the loading, in other words the higher the fraction of Keggin units being agglomerated, the more marked the band splitting. More marked means that the intensity at 1530 cm^{-1} increases relatively to that at 1540 cm^{-1} ($ratio_{1530/1540}$ of 0.60, 0.68 and 0.75 respectively at 35, 49 and 67% ML on Figure 4), and that the two maxima get better and better distinguished. It reflects that the fraction of pyridinium cations in the sample which lead to a split band increases. Thus, the higher the fraction of agglomerated Keggin units, the higher the fraction of pyridinium cations leading to a split band. This also appears as comparing the spectra of HPW12/P25 82% ML (Figure 2a) and HPW12/T805 67% ML (Figure 2b). Both show a split band, but the splitting is less marked in the case of the HPW12/P25 sample, although the latter has the highest loading among both. Indeed, according to Figure 1, the Keggin units are still much better dispersed in the HPW12/P25 sample than in the HPW12/T805 one. The fraction of agglomerated Keggin units is lower in the HPW12/P25 sample. So, in light of all these observations, the phenomenon responsible for the band splitting – most likely a tunneling effect associated to a frustrated rotation of the pyridinium cation (see Introduction) – occurs as a direct consequence of the agglomeration of HPW12

on the supports. In other words, the band splitting can be considered as a fingerprint of agglomerated HPW12.

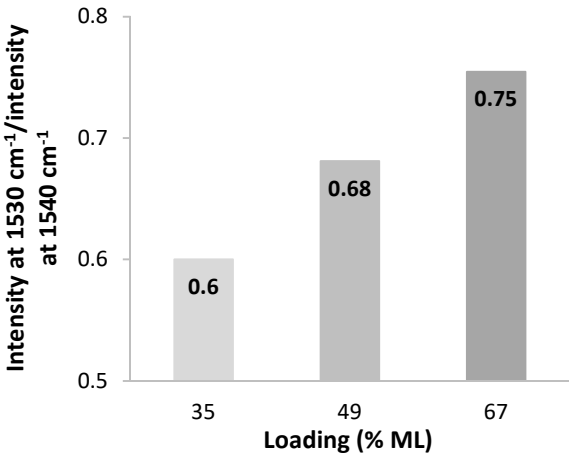

Figure 4. Ratio of the intensity at 1530 cm^{-1} over that at 1540 cm^{-1} within the ν_{19b} pyridinium ring vibration band observed for the HPW12/T805 samples as a function of the HPW12 loading. The IR intensities were all determined according to a baseline defined between 1560.2 and 1500.4 cm^{-1}.

Furthermore, by subtracting the spectrum of the pyridinium salt of pure HPW12 from those of pyridine adsorbed onto the supported samples, with a subtraction factor chosen to specifically eliminate the maximum/shoulder at 1530 cm^{-1} within the ν_{19b} pyridinium band (see an example on Figure 5), it is possible to directly access to the contribution of dispersed HPW12 to the latter band, and thereby to quantitatively estimate the fractions of both dispersed and agglomerated HPW12 within the supported samples (respectively by dividing the area of the band after subtraction by the initial area before subtraction, and by calculating the difference between 100 and the fraction of dispersed HPW12 to get the fraction of agglomerated HPW12, see values in Table 1). This represents a significant improvement compared to XPS which is unable to provide such quantitative information. Moreover, it can be applied to any kind of supported HPW12 sample, whatever the nature of the support. It facilitates the proper selection of samples to be used as catalysts, whatever the reaction. Indeed, as shown in reference[20], agglomerated Keggin units possess stronger acid sites than dispersed ones. Moreover, a given reaction might occur either only at the surface of the agglomerates or both at their surface and within their bulk. The latter mechanism applies, for example, in the case of the methanol-to-dimethylether reaction.[24] So, depending on the requirements in terms of acid strength and on the mechanism of the reaction, samples with a low, intermediate, or high fraction of agglomerated HPW12 should be selected as catalysts, and the innovative methodology reported here allows to easily make the right choice.

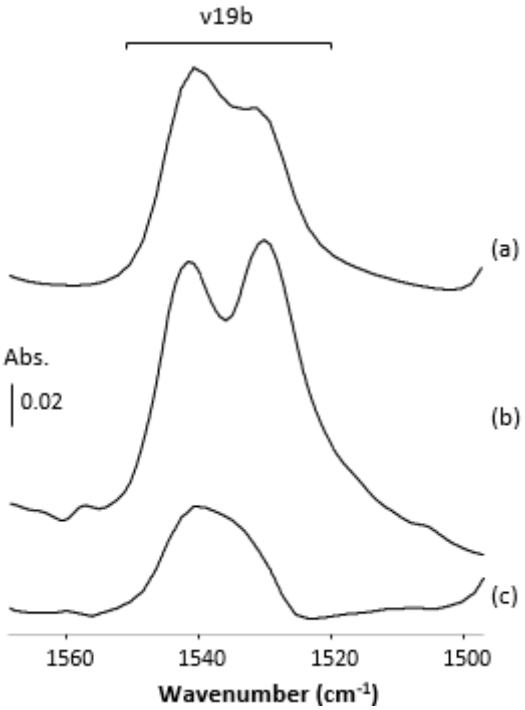

Figure 5. FT-IR spectra after exposure to pyridine of (a) HPW12/T805 67% ML and (b) pure HPW12, in the region of the ν_{19b} pyridinium ring vibration band. Spectrum (c) results from the subtraction "(a) – 0.4419 times (b)" to eliminate the maximum/shoulder at 1530 cm^{-1}, and shows thus the contribution of dispersed HPW12 exclusively.

Table 1. Fractions of dispersed and agglomerated HPW12 within the HPW12/P25 and HPW12/T805 samples determined thanks to the approach shown in Figure 5.

Support	Loading of HPW12 (% ML)	Fraction of dispersed HPW12 (%)	Fraction of agglomerated HPW12 (%)
P25	37	100	0
	66	100	0
	82	76	24
T805	35	70	30
	49	51	49
	67	38	62

The ν_{19b} pyridinium band splitting actually detects agglomerated HPW12 even better than XRD. Indeed, the latter detects here Keggin crystals only for the HPW12/T805 sample with 67% ML, namely the sample with the poorest HPW12 dispersion among all. In all other cases, the XRD patterns only show the diffraction lines of pure TiO_2, namely the same for P25 and T805 (see Figure 6 showing the patterns of the HPW12/T805 samples, and Figure S5 in the Supporting information showing the patterns of the pure materials – TiO_2 P25 and T805, and HPW12 – and of the HPW12/P25 samples). Indeed, although already agglomerated (but maybe not yet at an advanced state of agglomeration, for example due to the amount of HPW12 introduced in the formulation), Keggin units might not have formed ideal crystals yet, or the latter might still be too small to be detectable through XRD.[20]

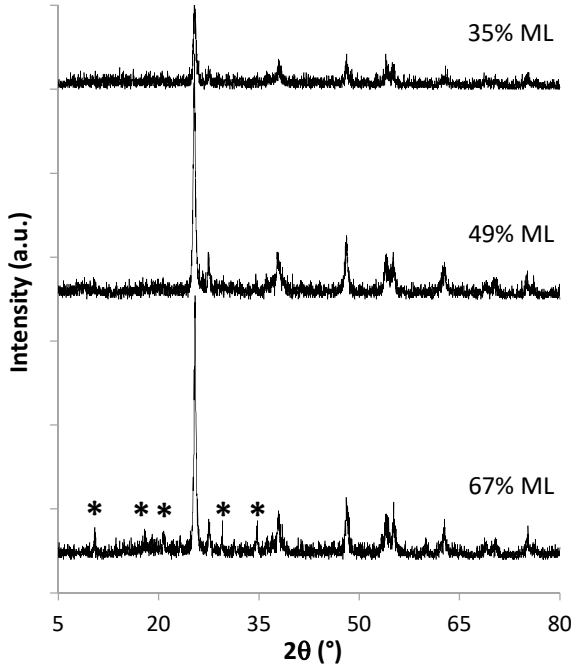

Figure 6. XRD patterns of the HPW12/T805 samples. Characteristic peaks of HPW12 crystals are marked with a star.

4. Conclusions

For the first time, the present paper shows that the ν_{19b} pyridinium IR band splitting well-known in the case of pure HPW12 actually also appears with supported HPW12, namely systematically in the presence of agglomerated Keggin units. More precisely, the higher the fraction of agglomerated Keggin units on the support, the more marked the band splitting, in other words the higher the fraction of pyridinium cations concerned by a tunneling effect associated in the literature to a frustrated rotation of the pyridinium cation within the solid bulk of HPW12 crystals. Thus, the latter phenomenon occurs as a direct consequence of the agglomeration of HPW12 on the support, what makes the pyridinium band splitting a powerful tool to probe the dispersion of supported HPW12. It is even more powerful than XRD which does not systematically detect Keggin crystals when pyridine-IR detects agglomerates, and it allows quantitatively evaluating the fractions of dispersed and agglomerated Keggin units within the supported samples. As the dispersion in general strongly influences the catalytic performance of HPW12, e.g. by dictating the strength and accessibility of the acid sites, this new approach facilitates the proper selection of samples to be used as catalysts, whatever the reaction, as a function of the reaction requirements.

Supporting information

Nominal and real (ICP-measured) HPW12 loadings (in weight fraction and in % ML) on both TiO_2 supports; N_2 physisorption isotherms of the pure supports; FT-IR spectra of HPW12/P25, HPW12/T805 and pure TiO_2 in particular conditions or spectral regions (with assignment of the bands related to TiO_2); XRD patterns of the HPW12/P25 samples and pure materials (TiO_2 P25 and T805, and HPW12).

Author information

Corresponding authors

*E-mail addresses: josischnee@hotmail.com, alexander.vimont@ensicaen.fr

Author contributions

J.S. and E.M.G. conceived the project of comparing the dispersion of HPW12 supported on TiO_2 P25 *vs.* T805; J.S. and A.V. conceived the project of investigating *in situ* FT-IR upon pyridine adsorption as a way to probe the dispersion of supported HPW12; J.S. was in charge of the sample preparation and *ex situ* characterization (at the Université catholique de Louvain during her PhD thesis), carried out the *in situ* FT-IR studies (at the Normandie Université/Laboratoire Catalyse et Spectrochimie during her post-doc) and wrote the manuscript; F.D. performed the XPS measurements (at the Université catholique de Louvain).

Conflicts of interest

The authors declare no competing interests.

Acknowledgements

The authors acknowledge Olivier Kallai for having, under the co-supervision of J.S. and E.M.G., contributed to the sample preparation and performed some of the *ex situ* characterization measurements in the framework of his Master thesis at the Université catholique de Louvain/Faculty of Bioengineering. J.S. acknowledges Prof. Marco Daturi (Normandie Université/Laboratoire Catalyse et Spectrochimie) for the post-doc position, and for his constructive comments on the manuscript.

Abbreviations

HPW12, $H_3PW_{12}O_{40}$ (phosphotungstic acid). % ML, percentage of the amount of Keggin units required to form one ideal monolayer on the support.

References

1. C. Binet, A. Travert, M. Daturi, J.-C. Lavalley and A. Vimont, *RSC Advances*, 2014, **4**, 19159-19164.
2. M. I. Zaki, M. A. Hasan, F. A. Al-Sagheer and L. Pasupulety, *Colloids and Surfaces A: Physicochemical and Engineering Aspects*, 2001, **190**, 261-274.
3. G. Busca, H. Saussey, O. Saur, J. C. Lavalley and V. Lorenzelli, *Applied Catalysis*, 1985, **14**, 245-260.
4. G. Busca, *Chemical Reviews*, 2007, **107**, 5366-5410.
5. I. V. Kozhevnikov, *Journal of Molecular Catalysis A: Chemical*, 2007, **262**, 86-92.
6. M. J. Janik, K. A. Campbell, B. B. Bardin, R. J. Davis and M. Neurock, *Applied Catalysis A: General*, 2003, **256**, 51-68.
7. H. Zhang, A. Zheng, H. Yu, S. Li, X. Lu and F. Deng, *J Phys Chem C*, 2008, **112**, 15765-15770.
8. R. M. Ladera, J. L. G. Fierro, M. Ojeda and S. Rojas, *Journal of Catalysis*, 2014, **312**, 195-203.
9. S. Akaratiwa and H. Niiyama, *Journal of Chemical Engineering of Japan*, 1990, **23** 143-147.
10. A. Małecka, J. Poźniczek, A. Micek-Ilnicka and A. Bielański, *Journal of Molecular Catalysis A: Chemical*, 1999, **138**, 67-81.
11. A. Micek-Ilnicka, *Journal of Molecular Catalysis A: Chemical*, 2009, **308**, 1-14.

12. T. Sugii, R. Ohnishi, J. Zhang, A. Miyaji, Y. Kamiya and T. Okuhara, *Catalysis Today*, 2006, **116**, 179-183.
13. A. Vimont, A. Travert, C. Binet, C. Pichon, P. Mialane, F. Sécheresse and J.-C. Lavalley, *Journal of Catalysis*, 2006, **241**, 221-224.
14. C. Pichon, P. Mialane, J. Marrot, C. Binet, A. Vimont, A. Travert and J.-C. Lavalley, *Physical Chemistry Chemical Physics*, 2011, **13**, 322-327.
15. J. G. Highfield and J. B. Moffat, *Journal of Catalysis*, 1984, **89**, 185-195.
16. N. Essayem, C. Lorentz, A. Tuel and Y. B. Tâarit, *Catalysis Communications*, 2005, **6**, 539-541.
17. R. M. Ladera, M. Ojeda, J. L. G. Fierro and S. Rojas, *Catal. Sci. Technol.*, 2015, **5**, 484-491.
18. W. Alharbi, E. F. Kozhevnikova and I. V. Kozhevnikov, *ACS Catalysis*, 2015, **5**, 7186-7193.
19. A. Popa, V. Sasca, E. E. Kiš, R. Marinković-Nedučin, M. T. Bokorov and J. Halasz, *Journal of Optoelectronics and Advanced Materials*, 2005, **7**, 3169-3177.
20. J. Schnee, A. Eggermont and E. M. Gaigneaux, *ACS Catalysis*, 2017, **7**, 4011-4017.
21. *Evonik Resource Efficiency GmbH*, 2018.
22. Z. Karimi, A. R. Mahjoub and S. M. Harati, *Inorganica Chimica Acta*, 2011, **376**, 1-9.
23. F. Thibault-Starzyk, B. Gil, S. Aiello, T. Chevreau and J.-P. Gilson, *Microporous and Mesoporous Materials*, 2004, **67**, 107-112.
24. J. Schnee and E. M. Gaigneaux, *Catalysis Science & Technology*, 2017, **7**, 817-830.

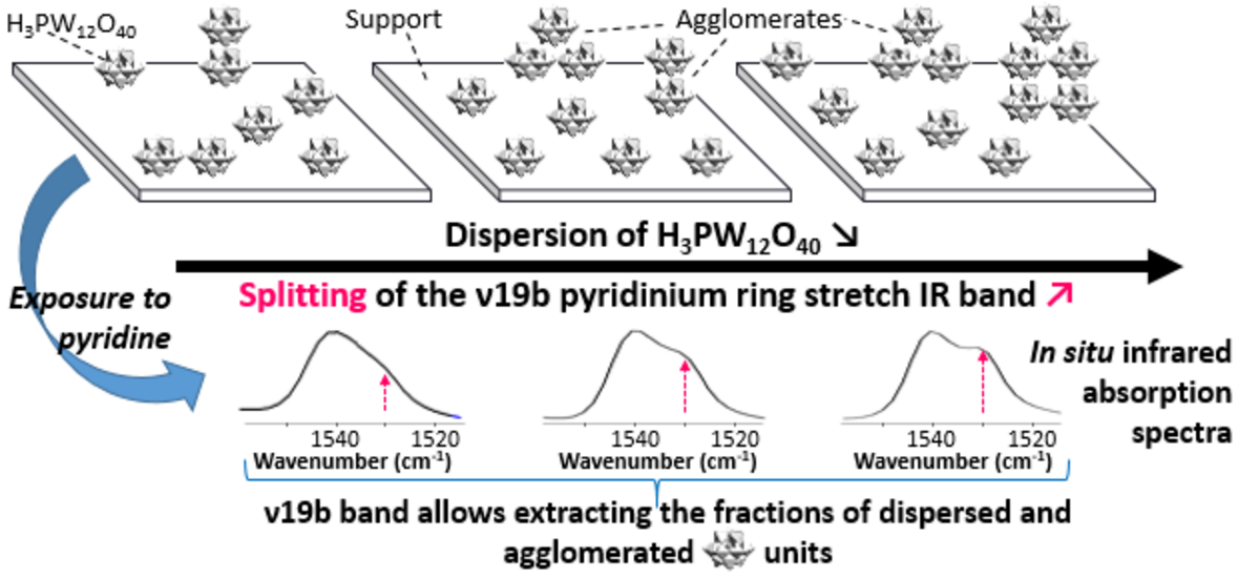
H3PW12O40
Support
Agglomerates
Dispersion of H3PW12O40 ↘
Exposure to pyridine
Splitting of the v19b pyridinium ring stretch IR band ↗
In situ infrared absorption spectra
1540
1520
Wavenumber (cm-1)
1540
1520
Wavenumber (cm-1)
1540
1520
Wavenumber (cm-1)
v19b band allows extracting the fractions of dispersed and agglomerated units